Analysis of Surface Crack Propagation Considering the Effect of Micro-separations

by

Junichi KATSUTA*, Kouji SAKAI**,
Kazuyoshi KAWANO* and Masaki NAKAJIMA*

In the TMCP steels rolled at the finishing temperature in austenite-ferrite region by the Non-AcC type TMCP method, it becames clear that the fatigue fracture surface had a lot of micro-separations, and fatigue crack propagation was prevented by micro-separations in the case of propagation in the direction of plate thickness.

In this study, the authors investigated on the behavior of surface crack propagation using three TMCP steels with different SI_{max}, and proposed the method of crack propagation analysis considering the effect of micro-separations.

The results may be summarized as follows:

(1) As SI_{max} increase, propagation pattern of surface crack become shallow.

(2) The macroscopic fatigue crack propagation can be analyzed with the assumption that the fatigue crack propagation in the direction of plate thickness passes through between estimated micro-separations.

(3) This estimation method shows the good agreement with the experimental change of aspect ratio for surface crack.

1. Introduction

Various researches on the fatigue strength and the fatigue crack growth rate of TMCP steels have been done, and it have became clear that the fatigue strength and the fatigue crack growth rate of TMCP steels are equal to those of conventional process steels. These researches, however, do not have mentioned the effect of separations occurred on fatigue fracture surface.

A part of the investigation regarding the effect of separations on the fatigue crack propagation behavior was already reported[1]. In this paper, it became clear that the fatigue fracture surface of TMCP steels with large maximum separation index (SI_{max}) had a lot of very small separations with length of 0.01~0.02mm in the direction paralleled to plate surface, and the fatigue crack propagation was prevented by very small separations in the case of propagating in the direction of plate thickness. Then, the very small separation affected fatigue crack propagation was named "micro-separation".

In this study, the authors investigated on the behavior of surface crack propagation using three TMCP steels with different SI_{max}, and proposed the method of crack propagation analysis considering the effect of micro-separations. Moreover we compared the experimental change of the aspect ratio with the estimated one using above the method of analysis.

2. Behavior of Surface Crack Propagation

2. 1 Materials and Experimental Method

Chemical composition, mechanical properties

Received April 30, 1991.
*Department of Structual Engineering
**Nippon Steel Corporation

and SI_{max} of test steels are shown in Table 1. These TMCP steels were produced from the same slab but were rolled at the different finishing temperatures in austenite-ferrite region by the Non-AcC type Thermo-Mechanical Control Process (TMCP). But each separation index (SI) on the fracture surface of Charpy impact test specimens of these TMCP steels is zero at room temperature.

Fig. 1 shows shapes of specimen used in the surface crack propagation test. In these specimens proposed by Kawahara et al.[2], there are equilibrated type and non-equilibrated type surface cracks. It is considered that the equilibrated type surface crack propagate from a small point defect in the plate surface, and the non-equilibrated type surface crack propagate from a shallow defect along the toe of weld bead.

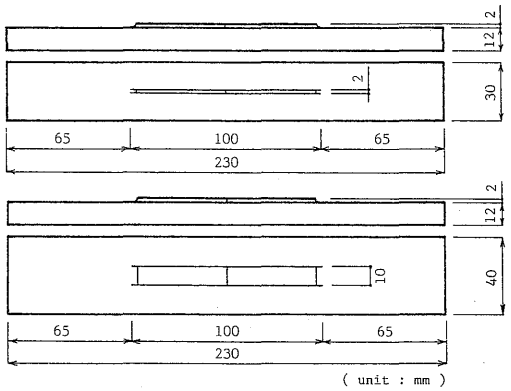

Fig. 1 Specimen configuration of surface crack propagation test

In order to investigate the effect of micro-separations on the surface crack propagation, experiments were carried out using the electric servo type fatigue testing machine under the conditions of cyclic loading speed 10Hz and stress ratio 0.1. The change of surface crack propagation pattern was measured by beach-mark occurred on the fatigue fracture surface under the conditions of fixing maximum load and changing stress ratio to 0.5.

2. 2 Results and Discussion

In the first step, the effect of SI_{max} on the fatigue crack growth rate was investigated.

Fig. 2 shows the relationships of crack growth rate (da/dn or dc/dn) to stress intensity factor

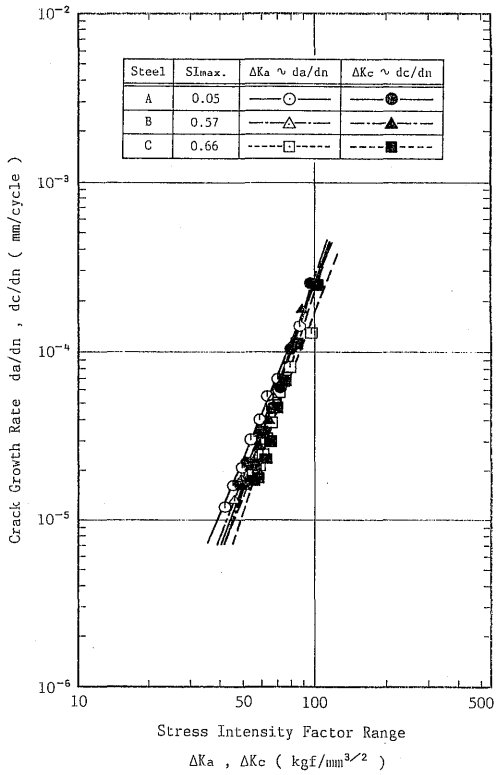

Fig. 2 Fatigue crack growth rate of equilibrated growth type surface crack

Table 1 Chemical composition, mechanical prperties and maximum separation index of test steels

Steel		Thickness (mm)	Chemical Composition (%)										Mechanical Properties			SI_{max}	T_{SImax} (°C)
			C	Si	Mn	P	S	Cu	Ni	Cr	Sol. Al	Ceq.**	Y.S. (kgf/mm²)	T.S. (kgf/mm²)	El. (%)		
LT*	A	25	0.12	0.36	1.44	0.013	0.002	0.01	0.02	0.02	0.076	0.366	38.5	51.1	28	0.05	-80
	B												43.6	55.0	24	0.57	-120
	C												42.5	53.8	25	0.66	-120

* : TMCP type Low Temperature Application Steel (SLA33B Equivalent)
** : Ceq. (IACS)=C+Mn/6+(Cr+Mo+V)/5+(Ni+Cu)/15

range (ΔK_a or ΔK_c) in the directions of depth and width of the equilibrated type surface crack. Fig. 3 shows the relations between crack growth rate and stress intensity factor range in the directions of depth and width of the non-equilibrated type surface crack. The stress intensity factor range was calculated by equation (1) of Newman-Raju[3].

$$\Delta K_a \text{ or } \Delta K_c = \Delta\sigma \cdot F \cdot \sqrt{\pi a/Q} \qquad (1)$$

In the equilibrated type surface crack, as may be seen from Fig. 2, any effect of SI_{max} on da/dn or dc/dn is not observed, and also there is almost no recognizable difference between da/dn and dc/dn, while in the non-equilibrated type surface crack, as shown in Fig. 3, and the effect of SI_{max} on dc/dn is not observed, but da/dn decrease as SI_{max} increase.

In order to compare with the results of surface crack propagation test, experiments on the fatigue crack propagation in the direction of plate width was carried out using specimen shown in Fig. 4 with center crack under above mentioned conditions. The length of fatigue crack occurred on the surface of specimen was measured by magnifying glass (×30). Results of this test are shown in Fig. 4. In order to obtain ΔK, following equation (2) was used.

$$\Delta K = \Delta\sigma \cdot F(a/W) \cdot \sqrt{\pi a} \qquad (2)$$

where, $F(a/W) = \sqrt{\sec(\pi a/2W)}$

2a : crack length

W : specimen width

Fig. 4 shows no effect of SI_{max} on da/dn, and these crack growth rates are almost the same as those in the direction of width in the equilibrated type and the non-equilibrated type surface cracks.

In the second step, the effect of SI_{max} on the change of surface crack propagation pattern was investigated.

Fig. 5 shows the relation between the aspect ratio of surface crack (a/c) and the ratio of surface crack

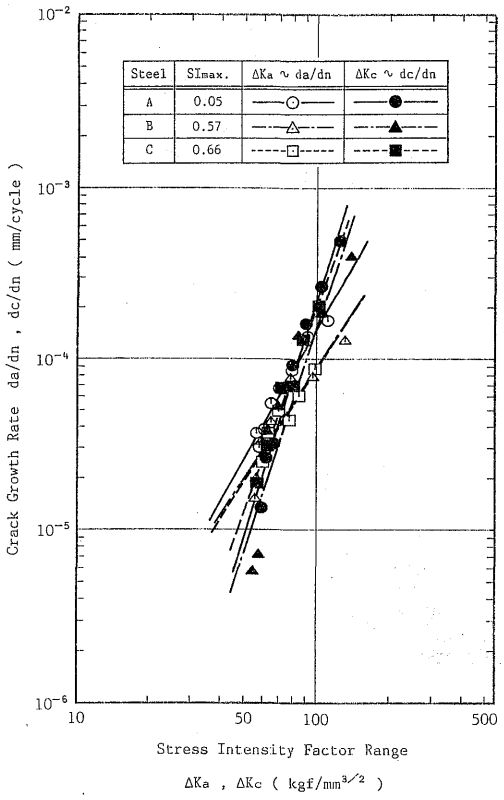

Fig. 3 Fatigue crack growth rate of non-equilibrated growth type surface crack

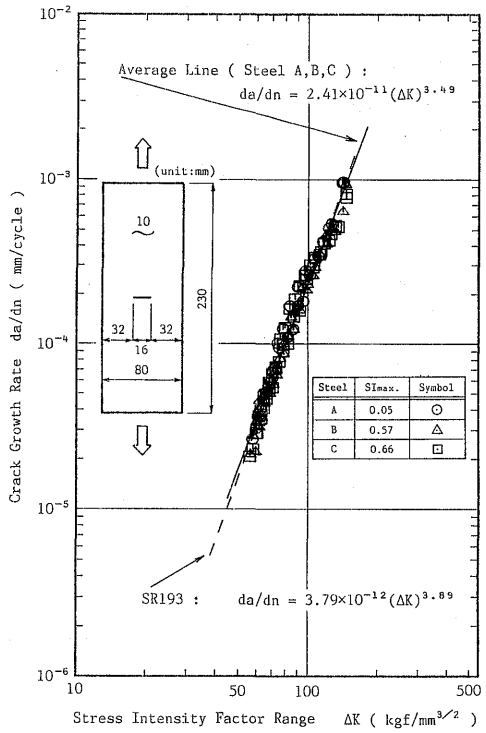

Fig. 4 Results of through thickness type fatigue crack propagation test

depth to specimen thickness (a/t) in the equilibrated type and the non-equilibrated type surface carcks. The propagation pattern of equilibrated type and non-equilibrated type surface cracks become shallow as SI_{max} increase.

Then, the effect of micro-separations on the propagation behavior of through thickness type fatigue crack in the direction of plate thickness was investigated. Cut-out method of specimen used in this test is shown in Fig. 6.

Fig. 7 shows the results of this test using specimen shown in this figure. As shown in Fig. 7, it is noticed that as SI_{max} increase, the crack propagation life increase, and though the same test condition and steel plate, the difference of crack propagation life increase in the steel with large SI_{max}.

The SEM fractograph of fatigue crack propagation test specimen is shown in Fig. 8. The existence of micro-separations paralleled to plate surface, is observed. It is considered that the micro-separations have the function to arrest fatigue crack propagation in the case of propagation in the direction of plate thickness.

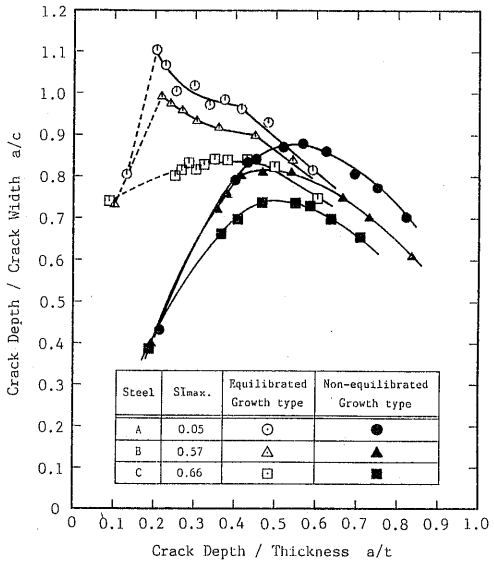

Fig. 5 Relation between a/t and a/c in surface crack propagation test

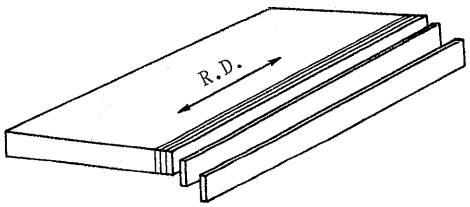

Fig. 6 Cut-out method of fatigue crack propagation test in the direction of thickness

3. Analysis of surface crack propagation

3. 1 Propagation analysis model

Under the assumption that the fatigue crack passes through between micro-separations in the semi-elliplical quasi-surface crack, as shown in Fig. 9, the investigation on the fatigue crack propagation pattern was performed using model test speci-

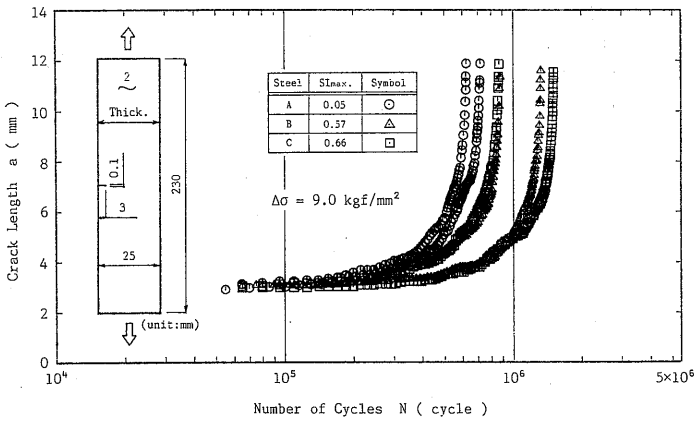

Fig. 7 Crack growth curves of propagation in the direction of thickness

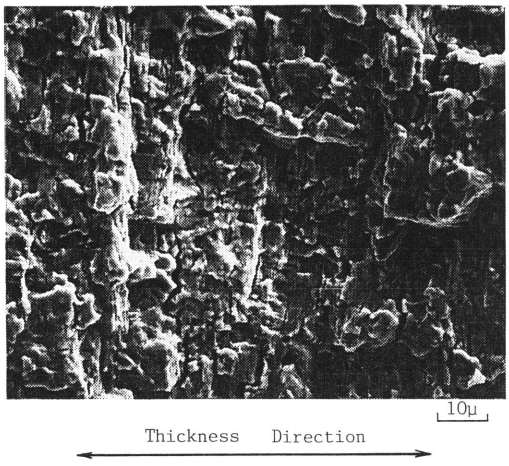

Fig. 8 SEM fractograph of Steel C ($\Delta\sigma$=9.0kgf/mm²)

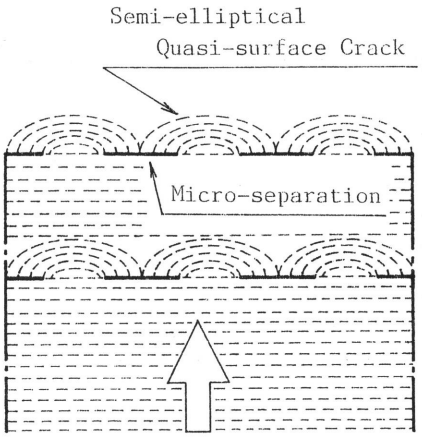

Fig. 9 Schematic diagram of fatigue crack to pass through between micro-separations

mens with surface slits paralleled to loading axis in which the fatigue crack passes through between slits.

Shape of specimens is shown in Fig. 10. Specimens were taken from Steel A in the rolling direction, therefore micro-separations do not affect the fatigue carck propagation in these specimens, because the fatigue carck propagate in the direction of plate width. Fig. 11 shows the relation between the required number of cycles (N_s) that the fatigue crack passes through between slits and the stress intensity factor range (ΔK) without consideration of the effect of slits. N_s tends to increase as the distance between slits and ΔK descrease.

The propagation analysis of crack which passed through between slits was carried out. The stress intensity factor range of semi-elliptical crack depth (ΔK_{sa}) was calculated by equation (1) of Newman-Raju, and the value (ΔK_p) was calculated by equation (3) of Kataza et al.[4]. ΔK_p is amount of influence of stress distributed over the part of through thickness crack on ΔK_{sa}.

$$\Delta K_p = 0.89\Delta K_{a1}\sqrt{a_t/\{\pi a(1-\xi_t^2)\}}\cdot F_s \qquad (3)$$

where, $a = a_t + a_s$, $\xi_t = 0.85\cdot a_t/a$

$$F_s = 1+(1+\xi_t)\cdot(0.2945-0.3912\xi_t^2+0.7685\xi_t^4 -0.9942\xi_t^6+0.5094\xi_t^8)$$

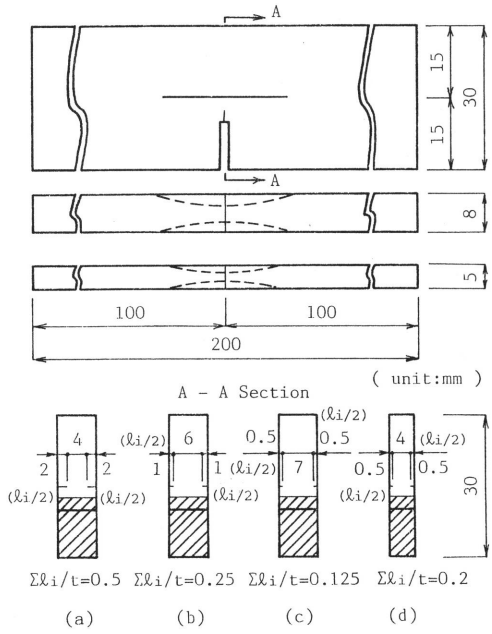

Fig. 10 Configuration of fatigue crack propagation test specimens with slits

ΔK_{a1} : stress intensity factor range at a_s=0

a_1 : length of through thickness type crack

a_s : depth of semi-elliptical quasi-surface crack

The required number of cycles to pass through

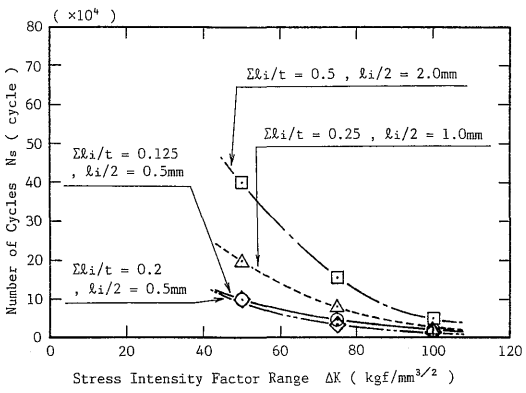

Fig. 11 Results of fatigue crack propagation test in the case of passage between slits

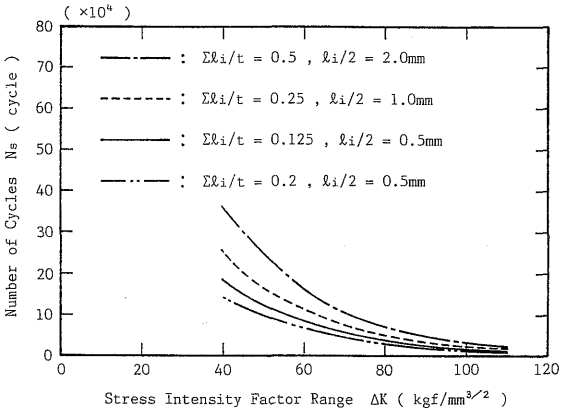

Fig. 12 Required number of cycles to pass through between slits in the calculation

between slits was obtained by integrating the stress intensity factor range of semi-elliptical quasi-surface crack depth (ΔK_{qa}) which was added ΔK_{sa} to ΔK_p. Moreover, in this caluculation, the average values shown in Fig. 4 were used for the coefficients (C, m) of Paris's low, and the propagation pattern of semi-elliptical quasi-surface crack was determined by experimental equation (4) of Kawahara et al.[2].

$$a_s = 1.17/(1/\sqrt{c_s^2 - c_{s0}^2} + 0.47/h) \qquad (4)$$

where, $h = W - a_l$

$2c_s$: length in the direction of width of semi-elliptical quasi-surface crack

$2c_{s0}$: distance between slits (length in the direction of width of initial semi-elliptical quasi-surface crack)

Fig. 12 shows the relationship between ΔK and N_s. And it shows that estimated N_s are smaller than experimental values, but N_s tends to increase as the distance between slits and ΔK become small in the same as experimental N_s. Therefore, the behavior of fatigue crack propagation considering the effect of micro-separations can be calculated by this assumption.

Using this method, the through thickness type fatigue crack propagation in the direction of plate thickness was calculated.

In this calculation, the following assumptions of the initiation behavior of micro-separations were made.

1) The crack contour line is straight without consideration of the effect of micro-separations.
2) Estimated micro-separations are initiated at the boundary of ferrite-pearite layers.
3) According to the measured results of width of ferrite and pearite layers, estimated micro-separations are initiated at every 0.007mm of crack propagation path.
4) Estimated micro-separations are initiated in terms of probabilities, and random variables are length and number of micro-separations.
5) The length of estimated micro-separation is determined by the probability density function of exponential distribution. (refer to Fig. 13)
6) Numbers of estimated micro-separation are determined by the probability density function of Weibull's distribution. (refer to Fig. 14)
7) Estimated micro-separations are distributed to crack contour line uniformly.
8) As shown in Fig. 15, propagation patterns of the semi-elliptical quasi-surface crack which arrive at the initiated position of next estimated micro-separation are calssified according to the cases that next estimated micro-separations exist (type A) or not (type B) at the tip of depth a_s of quasi-surface crack. That is to say, in type A, the propagation in the direction of depth of quasi-surface crack is arrested and the propaga-

tion in the direction of width of the crack advances till the crack combine with neighboring cracks. And in type B, the next quasi-surface crack starts to propagate neglecting propagation in the direction of width of the crack.

Table 2 shows the classified criterions of these propagation patterns determined by the ratio of estimated micro-separation numbers ($R_{g,i}=N_{g,i}/N_{g,i-1}$) and the ratio of estimated micro-separation length ($R_{l,i}=l_i/l_{i-1}$). Values of above $R_{g,i}$ and $R_{l,i}$ are obtained by deawing the relative position of quasi-surface crack contour line to estimated micro-separations.

The analysis of through thickness type crack propagation considering the effect of micro-separations was carried out on the assumption that the crack passes through between micro-separations. Fig. 12 shows the distribution of probability density of pearite structure length, and Fig. 13 shows the distribution of probability density of

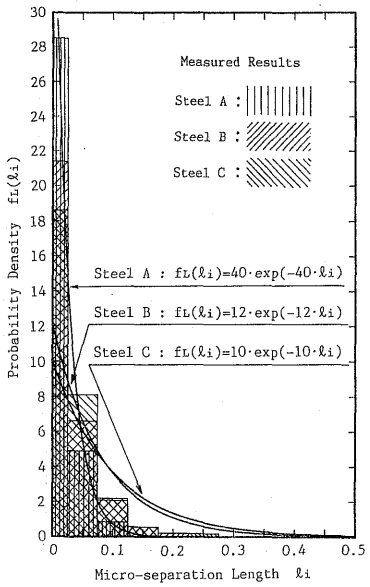

Fig. 13 Probability density of micro-separation length

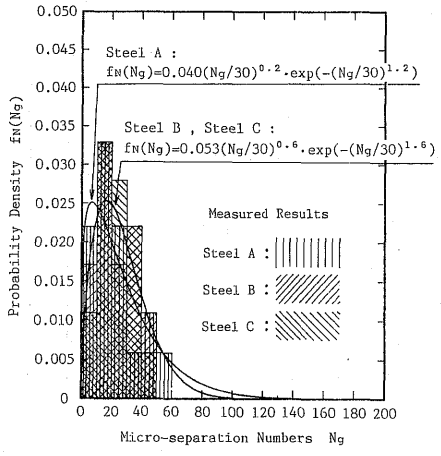

Fig. 14 Probability density of micro-separation numbers

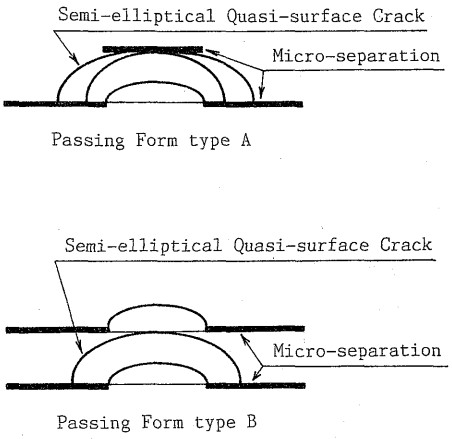

Fig. 15 Schematic diagrams of propagation pattern

Table 2 Classified criterions of propagation pattern for crack propagation analysis

Condition	Passing Form Between Micro-separations			
$R_{g,i}\leqq 0.2$	$l_i<0.2$	B	$l_i\geqq 0.2$	A
$0.2<R_{g,i}<0.8$	$R_{l,i}<4.0$	B	$R_{l,i}\geqq 4.0$	A
$0.8\leqq R_{g,i}\leqq 1.2$	$R_{l,i}<4.0$	B	$R_{l,i}\geqq 4.0$	A
$1.2<R_{g,i}<1.5$	$R_{l,i}<2.0$	B	$R_{l,i}\geqq 2.0$	A
$1.5\leqq R_{g,i}<1.8$	$R_{l,i}<1.0$	B	$R_{l,i}\geqq 1.0$	A
$1.8\leqq R_{g,i}\leqq 2.2$	$R_{l,i}>0.25$	A	$R_{l,i}\leqq 0.25$	B
$2.2<R_{g,i}<2.5$	$R_{l,i}<2.0$	B	$R_{l,i}\geqq 2.0$	A
$2.5\leqq R_{g,i}<2.8$	$R_{l,i}<1.0$	B	$R_{l,i}\geqq 1.0$	A
$2.8\leqq R_{g,i}\leqq 3.2$	$R_{l,i}<2.0$	B	$R_{l,i}\geqq 2.0$	A
$3.2<R_{g,i}<3.8$	$R_{l,i}<1.0$	B	$R_{l,i}\geqq 1.0$	A
$3.8\leqq R_{g,i}\leqq 4.2$	$R_{l,i}>0.5$	A	$R_{l,i}\leqq 0.5$	B
$4.2<R_{g,i}<4.8$	$R_{l,i}<1.0$	B	$R_{l,i}\geqq 1.0$	A
$4.8\leqq R_{g,i}$	$l_i>0.01$	A	$l_i\leqq 0.01$	B

$R_{g,i}=N_{g,i}/N_{g,i-1}$
$R_{l,i}=l_i/l_{i-1}$
$N_{g,i}$: Number of Micro-separations
li : Length of Micro-separation

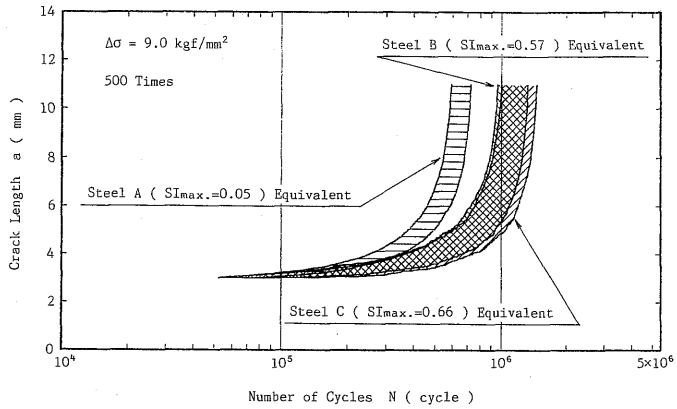

Fig. 16 Results of through thickness type crack propagation analysis condidering the effect of micro-separations

pearite structure numbers because micro-separations are supposed to generate the boundary of ferrite and pearite structures in the vicinity of a crack tip as a crack propagates. The coefficients of probability density functions in Figs. 12 and 13 were obtained from the probability papers plotted the probability of length and numbers of pearite structures. Fig. 16 shows the range of through thickness type crack propagation curves in the results of analysis considering the effect of estimated micro-separations. It shows that the crack propagation life increases as the micro-separations increase, and though the same analysis condition and micro-separation values, the difference of crack propagation life increases as the micro-separations increase in the same as the results of experiment.

Therefore, this method of crack propagation analysis considering the effect of micro-separations do not reproduce exactly the behavior that crack passes through between micro-separations, but it is considered that the behavior of the macroscopic crack propagation in the case of initiating micro-separations, can be understood by this analysis method.

3. 2 Results of calculation and Discussion

The effect of micro-separations on the aspect ratio of surface crack is investigated by the results of calculation considering the effect of micro-separations.

The change of aspect ratio of calculation and experimental results are shown in Fig. 17. It is noticed that the estimated aspect ratio tends to become shallow as SI_{max} increases in the same as the experimental one. But, there is the difference between the estimated aspect ratio and the experimental one. It is considered that the effect of convexity appears in the experimental aspect ratio.

Then, Fig. 18 shows the aspect ratio of non-equilibrated growth type surface crack of Steel A with or without consideration of the effects of micro-separations and convexity. The estimated aspect ratios considering the effect of micro-separations are plotted by hollow symbols, and the estimated aspect ratios considering the effects of micro-separations and convexity are plotted by solid symbols. The estimated result (thick line) without consideration of the effects of micro-separations and convexity by Kataza's equation[4], and the experimental result (thin line) obtained by this study are shown together in this figure. From this figure, it is clear that the estimated aspect ratio considering the effects of micro-separations and convexity agree approximately with the experimental aspect ratio, and the estimated aspect ratio considering the effect of micro-separations become shallower than the estimated aspect ratio without consideration of the effect of micro-separations in the case of no effect of convexity.

Fig. 19 shows the estimated aspect ratio considering the effects of micro-separations and convexity. The symbols indicate the estimated aspect ratio, and the lines indicate the experimental one. As shown in this figure, the estimated aspect ratio agree almost with the experimental one. It is considered that a slight difference between the estimated aspect ratio and the experimental one come out because micro-separations are initiated in a statistical manner.

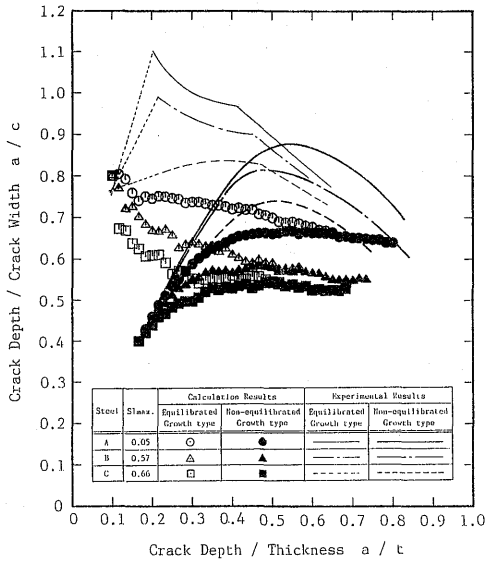

Fig. 17 Relation between a/t and a/c in surface crack propagation analysis considering the effect of micro-separations

Fig. 20 shows the relation between crack growth rate and the stress intensity factor range in the directions of depth and width of equilibrated type and non-equilibrated type surface cracks which are analyzed with consideration of the effect of micro-separations. In this figure, the experimental crack growth rates of through thickness type crack propagation in the directions of plate thickness and width are shown by lines. As shown in this figure, the calculated crack growth rate agree with the experimental one.

As the above investigated results show, it becomes clear that the macroscopic propagation behavior of surface carck can be estimated by the calculation method presented in this study.

4. Conclusions

The effect of SI_{max} on the propagation behavior

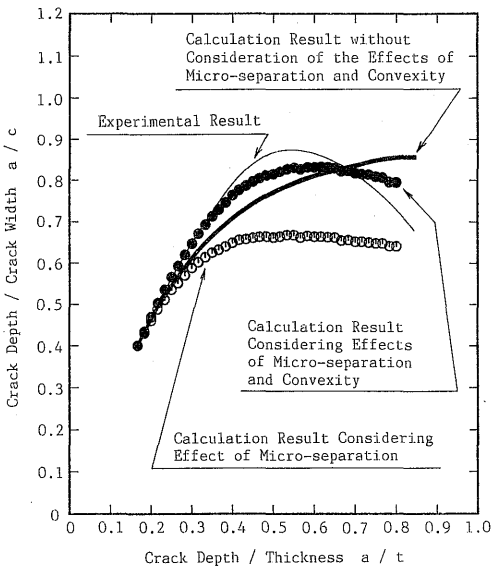

Fig. 18 Calculation results of change of aspect ratio with/without consideration of the effects micro-separations and convexity (Steel A, Non-equilibrated growth type surface crack)

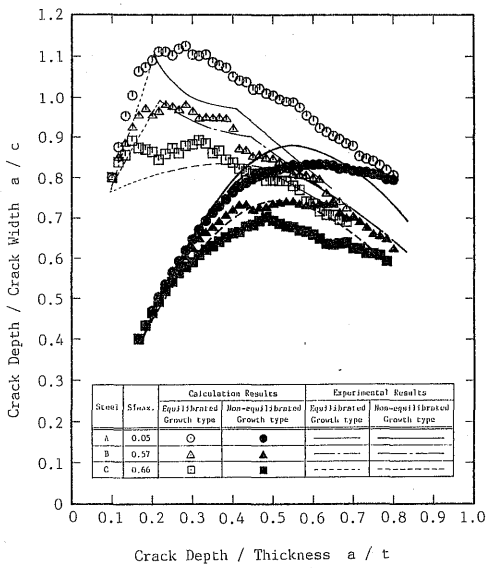

Fig. 19 Estimated change of aspect ratio considering the effects of micro-separations and convexity

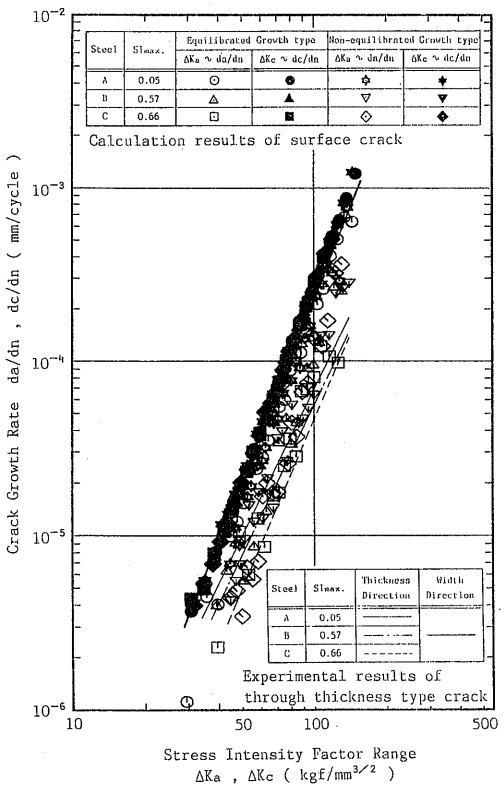

Fig. 20 Macroscopic crack growth rate plotted to ΔK value for each direction

of surface crack is investigated using three TMCP steels with different SI_{max}. And, the authors proposed an estimation method of surface crack propagation for steel plates in which micro-separations were initiated. The conclusions are as follows;

(1) As SI_{max} increase, propagation pattern of surface crack become shallow.

(2) The macroscopic fatigue crack propagation in the direction of plate thickness can be analyzed with the assumption that the fatigue crack passes through between estimated micro-separations.

(3) This estimation method shows the good agreement with the experimental change of aspect ratio for surface crack.

References

1) J. Katsuta and M. Nakajima ; On the Propagation of Fatigue Crack with Occurrence of Micro-separation, The West-Japan Socuety of Naval Architects, No. 76, 1988

2) M. Kawahara and M. Kurihara ; A preliminary Study on Surface Crack Growth in a Combined Tensile and Bending Fatigue Process, Journal of the Society of Naval Architects of Japan, Vol. 137, 1975

3) J. C. Newman and I. S. Raju ; An Empirical Stress-intensity Factor Equation for the Surface Crack, Engineering Fracture Mechanics, Vol. 15 No. 1-2, 1981

4) T. Kataza et al. ; A proposal of Fracture Control Design Procedure, Journal of the Society of Naval Architects of Japan, Vol. 149, 1981